

CR

74

Loan Copy

3

Illinois State Water Survey

at

University of Illinois
Urbana, Illinois

RADAR ANALYSIS OF PROJECT WARM RAIN
HILO, HAWAII - SUMMER, .1965

by

R. G. Semonin
E. A. Mueller
G. E. Stout
D. W. Staggs

Final Scientific Report

on

NSF Grant GP-194

Prepared for

National Science Foundation

February 17, 1967

CONTENTS

	Page
ABSTRACT.	i
INTRODUCTION.	1
RADAR CHARACTERISTICS.	2
M-33.	2
GPG-1.	3
RADAR OBSERVATIONS AND ANALYSIS.	4
M-33.	4
Echo Frequency versus Rainfall.	7
Echo Diameter Frequency versus Range.	8
Initial Echo - Movement and Origin.	10
Typical Echo Morphology and Special Cases.	11
GPG-1.	13
SUMMARY.	14
RECOMMENDATIONS.	15
ACKNOWLEDGMENTS.	16
REFERENCES.	17
APPENDIX 1	
Precipitation Log near University of Hawaii, Hilo Campus	
APPENDIX 2	
M-33 -- Summary of Operations	

ABSTRACT

Two X-band radar sets, an M-33 and a GPG-1, were operated routinely on the island of Hawaii during the period July 11 through August 28, 1965. The primary function of these operations was to support the concerted effort of cloud physicists from Japan and the United States to obtain data on the warm rain mechanism.

The M-33 was located at the Cloud Physics Observatory on the Hilo campus of the University of Hawaii. The data obtained from the PPI scope photography were used to determine preliminary climatological parameters associated with trade wind showers.

The relationship between echo frequency and rainfall was examined and found to be remarkably good. These results show that the rainfall rate during the data collection period was very uniform. Such an analysis is useful in the determination of rainfall amounts over the ocean and over the land in the vicinity of Hawaii where the rain gauge density is sparse.

The frequency of echoes of a given diameter as a function of range was tabulated according to whether the echo was observed over land or over water. It is apparent from these data that there was a greater frequency of echoes per unit area over land than over water. This is attributed to the breakup of organized lines or bands of showers as they moved inland. In addition, there is a distinct decrease of echo frequency with increasing range. The observed decrease of echo frequency cannot be accounted for by range attenuation or atmospheric refraction.

The relationship between echo movement and the trade winds was studied. The results indicate that the radar echoes tend to move to the right of the wind direction with a greater speed than the environmental wind.

Selected examples of radar photographs are presented which illustrate typical echo displays. In addition, the radar presentation of a mesosystem and the echoes associated with a Hawaiian thunderstorm are shown.

The GPG-1 radar was located at 2100 meters on the windward slope of Mauna Kea. Very little useful data were obtained from this location due to trapping gradients associated with the trade inversion. An example is shown where the propagation path was extended and the sensitivity reduced by refractive index gradients. The site was abandoned early in the project in favor of a more concentrated effort on the M-33 operations.

INTRODUCTION

In the Fall of 1963, the Atmospheric Sciences Section of the Illinois State Water Survey at the University of Illinois was invited to act as the U. S. counterpart to a proposal from Dr. K. Isono of the Water Research Laboratory of Nagoya University concerning field observations of the precipitation process in Hawaii. Since there are a number of groups in the U. S. that are interested in performing studies of the all-water precipitation mechanism, a one-day conference in Chicago was sponsored by the National Center for Atmospheric Research (NCAR) to bring together a group of cloud physicists who could provide information on Hawaiian rainfall from previous experience or who might be interested in direct participation.

The meeting was quite useful and laid the foundations for submission of a research proposal to the National Science Foundation. During the ensuing 11 months a proposal was prepared and a trip to Hawaii was made to bring together the scientists from Japan and the United States for the purpose of locating field sites and discuss in detail the work to be accomplished. The on-site inspection of facilities in Hilo, Hawaii, jointly with the Japanese and other participants from the United States was very useful to the future conduct of the project.

In brief, there were three locations chosen as sites for the various radars, a balloon launching platform, and the field headquarters for the Japanese. The elevations for these sites were 56, 780, and 2100 meters above sea level. This report will be concerned with the M-33 radar operations at the 56 meter level (Cloud Physics Observatory (CPO), Hilo Campus, U. of Hawaii) and the GPG-1 radar operations at the 2100 meter level on Mauna Kea. These locations are indicated in Figure 1.

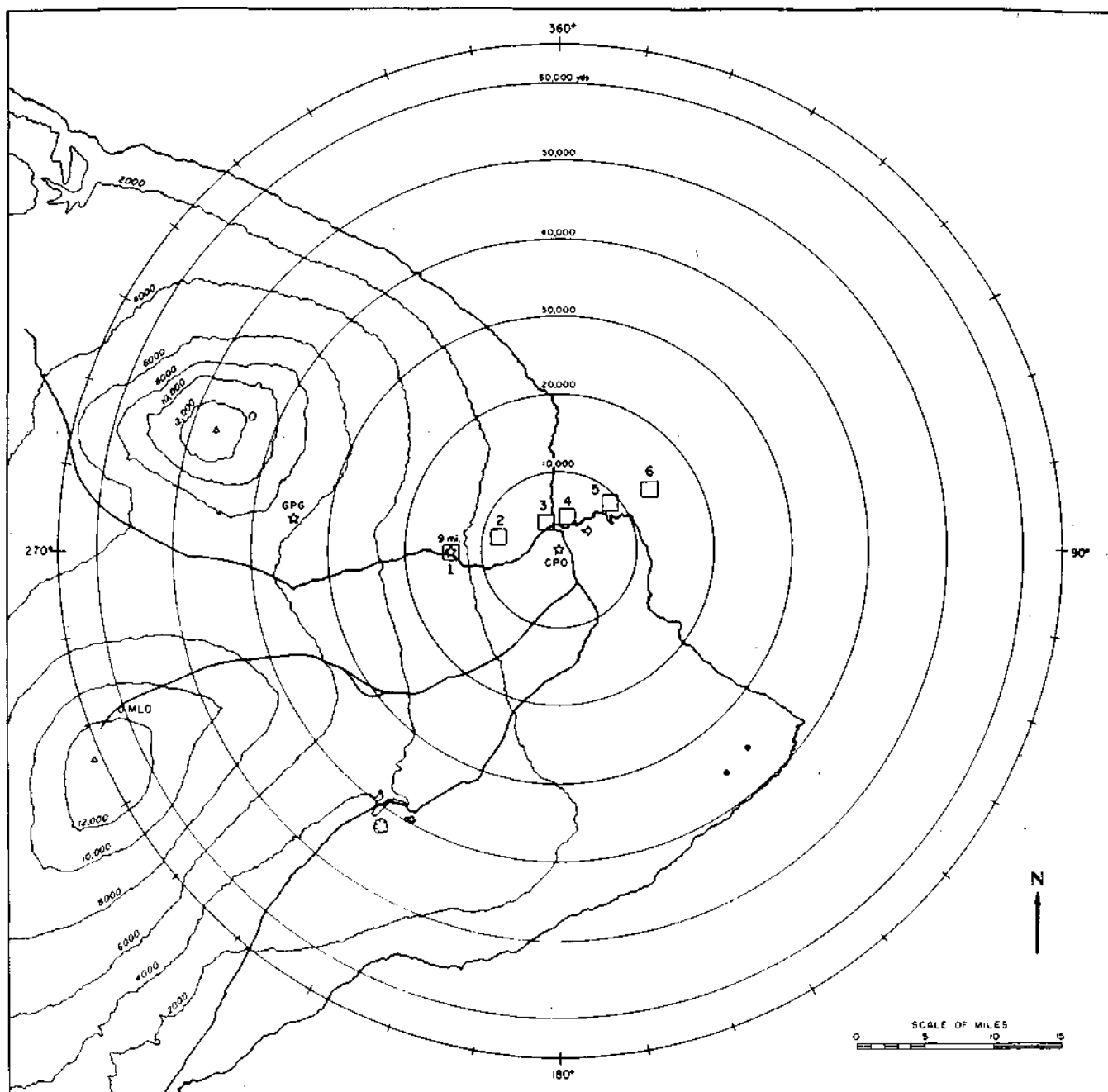


Figure 1. Radar locations and the Japanese balloon launching site on the east side of the island of Hawaii

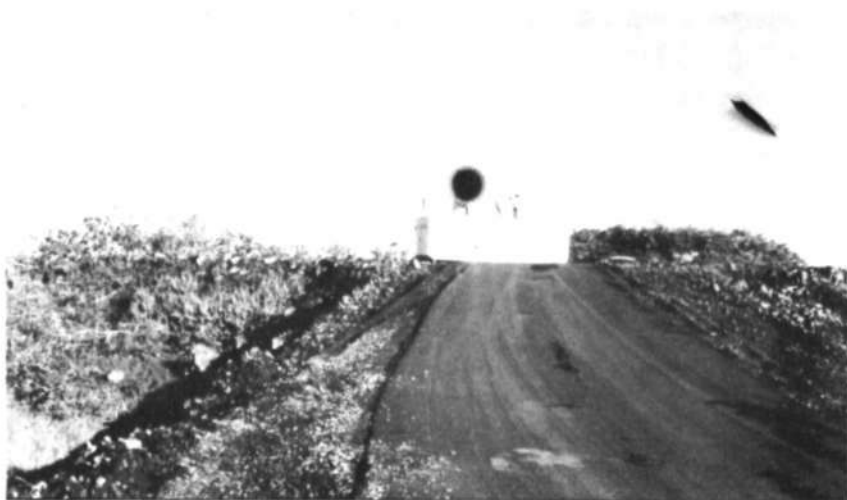
RADAR CHARACTERISTICS

M-33

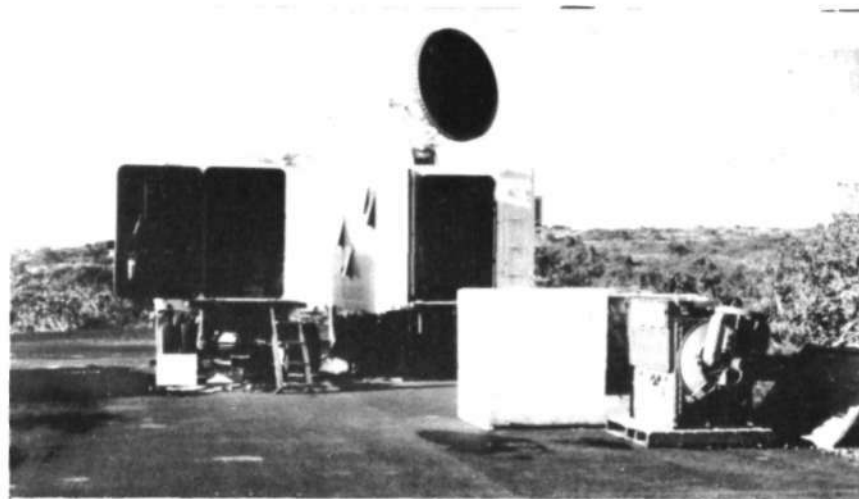
Two radars were used by the Water Survey on this project. The primary radar used for data collection was the tracking radar of an M-33 system supplied by NCAR. This radar, shown in Figure 2, was located at the CPO. The radar was equipped with a step gain control, an antenna elevation control, and a Survey-owned 35-mm camera. These controls were designed by Water Survey personnel which were then constructed and installed by NCAR. The step gain control provided for two modes of operation. In one mode the nominal difference in sensitivity of two adjacent steps was 4db. In mode 2 the difference was about 8db.

The antenna operating mode allowed the elevation angle to be programmed. There were 10 elevation angles plus two types of 0° (horizontal) operation incorporated into the antenna mode programmer. In one type of 0° operation (commonly referred to as split-Z), the antenna was held at 0° through the eastern semicircle (ocean area) and was raised to about $4\frac{1}{2}^\circ$ through the western semicircle (land area). This elevation in the western sector allowed the radar to look above the majority of the ground return from the mountain slopes. This technique proved valuable and most of the routine data were taken with this mode of operation. In addition to these changes in the antenna drive system, NCAR provided a modification of the range of the PPI scope and added range marks.

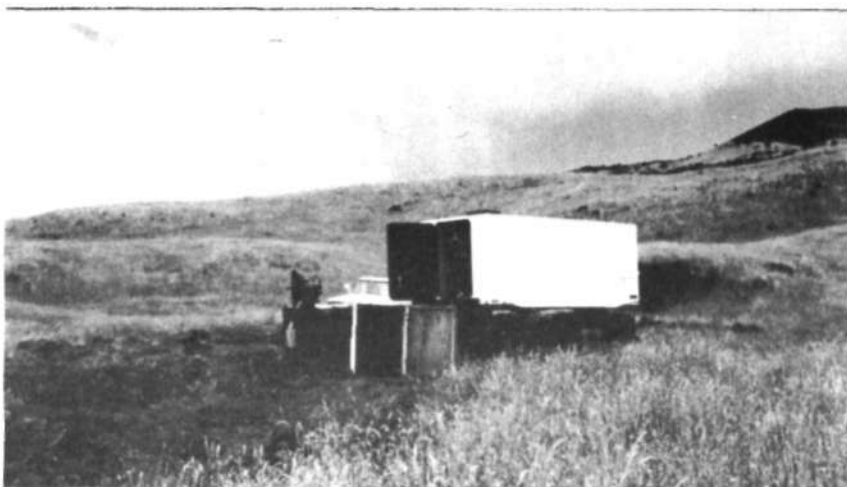
The M-33 radar was installed at the CPO in early June and was in an operating condition, except for camera circuit difficulties, by June 15. The radar was calibrated using a 10 inch diameter metallic sphere flown on a Jalbert wing on two occasions. These two calibrations, which agree to within 2db were made on July 9 and on August 20, 1965. Table 1 contains the measured characteristics and



a) M-33 at the Cloud Physics Observatory with the cloud camera on top of the van.



b) The M-33 and GPG-1 radars on the radar pad.



c) The GPG-1 and maintenance van at the 2100 meter level on Mauna Kea.



d) A view toward the 9-mile station from the GPG-1 radar site.

Figure 2. The M-33, X-band tracking radar and the GPG-1, X-band radar on location.

nominal characteristics of the radar. The transmitter power was always operated at lower than rated values. Receiver sensitivities were generally high for this type of radar.

Table 1. Characteristics of the M-33 Radar

<u>Characteristic</u>	<u>Nominal Value</u>	<u>Measured Value</u>
Peak transmitter power	250 Kw	80 to 175 Kw
Pulse repetition frequency	1500 Hz	1465 Hz
Pulse length	75 m	75 m
Antenna gain	39 db	37 db
Antenna 1/2 power beam widths	$20 \cdot 10^{-3}$ rad	-
Receiver sensitivity (MDS)	-97 dbm	-96 to -101 dbm
Frequency	8500-9600 MHz	9065 MHz

The crystal detectors used in the receiver were better than those for which the set was originally designed. The nominal receiver sensitivity of -97dbm was calculated assuming the stated noise figure for the receiver of 12.5db and that a coherent signal can be seen 6db below the average power of the noise. The two independent measures of overall performance using the metallic spheres yielded values for antenna gain of 36db and 38db.

GPG-1

The second radar, the X-band GPG-1, was planned to augment the M-33 during times of balloon tracking. The GPG-1 was also capable of tracking operation for short ranges. This radar, shown in Figure 2, was installed along the Humuula Sheep Station road at 2100 meter mean sea level elevation. The radar was moved into place on June 17 and was in operating condition by July 5.

Considerable modifications were made on the GPG-1 by the State Water Survey before shipment to Hawaii. These consisted of changing the pulse repetition frequency, changing the azimuth drive system, the installation of an automatic stepping switch, the installation of an antenna mode programmer, the installation of a VE-1 repeater scope and camera for data recording, and the installation of strip chart recorders to record antenna angles when in the tracking mode. These modifications were successful but little data were collected with this radar due to the undesirable atmospheric conditions part of the time at the location. A metallic sphere calibration was made on this radar and yielded an antenna gain of 31db. The characteristics of the GPG-1 are shown in Table 2.

Table 2. Characteristics of the GPG-1 Radar

<u>Characteristic</u>	<u>Nominal Value</u>	<u>Measured Value</u>
Peak transmitter power	40 Kw	22 Kw
Pulse repetition frequency	3800 Hz	3900/975 Hz
Pulse length	75 m	75 m
Antenna gain	-	31 db
Antenna 1/2 power beam widths	$52 \cdot 10^{-3}$ rad	-
Receiver sensitivity (MDS)	-90 dbm	-92 dbm
Frequency	8400-9600 MHz	8780 MHz

RADAR OBSERVATIONS AND ANALYSIS

M-33

The primary purpose of the radar facility was to provide the other investigators with information and prognostications related to the development and movement

of showers imbedded in the trade winds. These predictions were used by the Japanese and others to prepare various sampling instruments for data collection. For example, three of the Japanese scientists, according to a schedule, released radiosonde instruments for the measurement of drop size, drop electrical charge, and cloud water pH. The exact moment of release of a balloon was predicated upon radar information. In addition, the radar was used as a tracking device for the drop-charge radiosondes, whereas for the drop-size and pH radiosondes the radar was operated in the CAPPI mode with varying gain steps.

During periods of fine weather, zero-lift balloons were released by personnel of the University of Hawaii for the purpose of studying the air flow over the island of Hawaii. The M-33 was used in the tracking mode to follow the balloons which carried a radar reflector. The results from a limited number of flights were described by Lavoie (1966).

The chemical analysis of rainwater in relation to the age of the shower was attempted by personnel of the University of Hawaii. The plan for data collection involved tracking an individual shower which moved along one of the three highways noted in Figure 1. The M-33 radar operator, by means of radio communication, notified mobile collection units to proceed to previously agreed coordinates. The information desired from the radar concerning the showers included the speed and direction of movement, the relative position of the collection units to the shower, and the morphological history of the shower. Some difficulty was encountered in collecting data since the true nature of the showers did not fit the idealized model discussed in briefings. On a few occasions the mobile units were contacted, but the relative position of the radar echo to the units was not satisfactorily reconciled.

A limited number of attempts were made to observe the development of trade-wind showers in a manner similar to that described by Saunders (1965). During

periods when the showers were dispersed over a large area and were sufficiently sparse that they were considered independent, the individual showers were scanned for the maximum reflectivity with the M-33 in the tracking mode. In most of the instances when the technique was tried the maximum reflectivity was observed at some upper level within the cloud. However, the automatic tracking of this part of the cloud was not very successful. The M-33 would track for a variable length of time (minutes) and then arbitrarily seek another nearby target that for one reason or another presented a more desirable reflectivity. The results from these attempts showed that the plan-tracking of the direction of the echoes agreed reasonably well with the radiosonde and pibal observations of the trade wind structure. This technique could be valuable in studies relating to the motion of the showers as well as to determinations of the lifetimes of individual echoes. The technique, as attempted, was not useful for the measurement of the fall velocity of the maximum reflectivity volume of the cloud, and hence could not provide any information concerning the collection process in the trade-wind clouds.

The radar climatological data obtained during the pursuance of the major goals of the project were somewhat limited, but certain generalizations appear to apply to the observations made during the summer of 1965. Most of the data can be categorized into four types of radar presentations, that is, scattered showers, line showers, orographic rain, and Kona thunderstorms.

The synoptic weather coinciding with each of these types was examined to determine whether the stratification of the observations was uniquely determined by large scale meteorological features. Unfortunately, except in extreme and obvious cases, there were no readily apparent synoptic patterns that would uniquely determine the radar type.

The analyses presented in this report consist of the relationships between echo frequency and rainfall, echo diameter frequency and range, first echo development and movement, and a discussion of typical and special cases which occurred during the program. Continued observations with the radar at Hilo should strengthen the preliminary results and observations reported in this paper.

Echo Frequency versus Rainfall. A series of six one-nautical-mile squares were constructed on an acetate overlay as shown in Figure 1. The squares were aligned in the direction of the prevailing trade winds. The occurrence or non-occurrence of echoes in any of the squares was tabulated for nearly 212 hours of radar photographs acquired throughout the summer field program. No attempt was made to separate the data by hour of the day, intensity of echo, or synoptic conditions.

The rainfall was estimated for each of the squares from the data presented by Lavoie (1966). The results from this study are summarized in Table 3.

Table 3. Echo Frequency versus Rainfall

<u>Location</u>	<u>Rainfall (inches)</u>	<u>Echo Frequency (number)</u>
1	15.5	167
2	16.0	233
3	15.0	150
4	13.0	99
5	9.0	67
6	7.8	72

When the data are normalized by taking the ratio of the number of echo occurrences to the total rainfall and plotting the resulting number versus the echo occurrences, the relationship shown in Figure 3 is obtained. The two open-

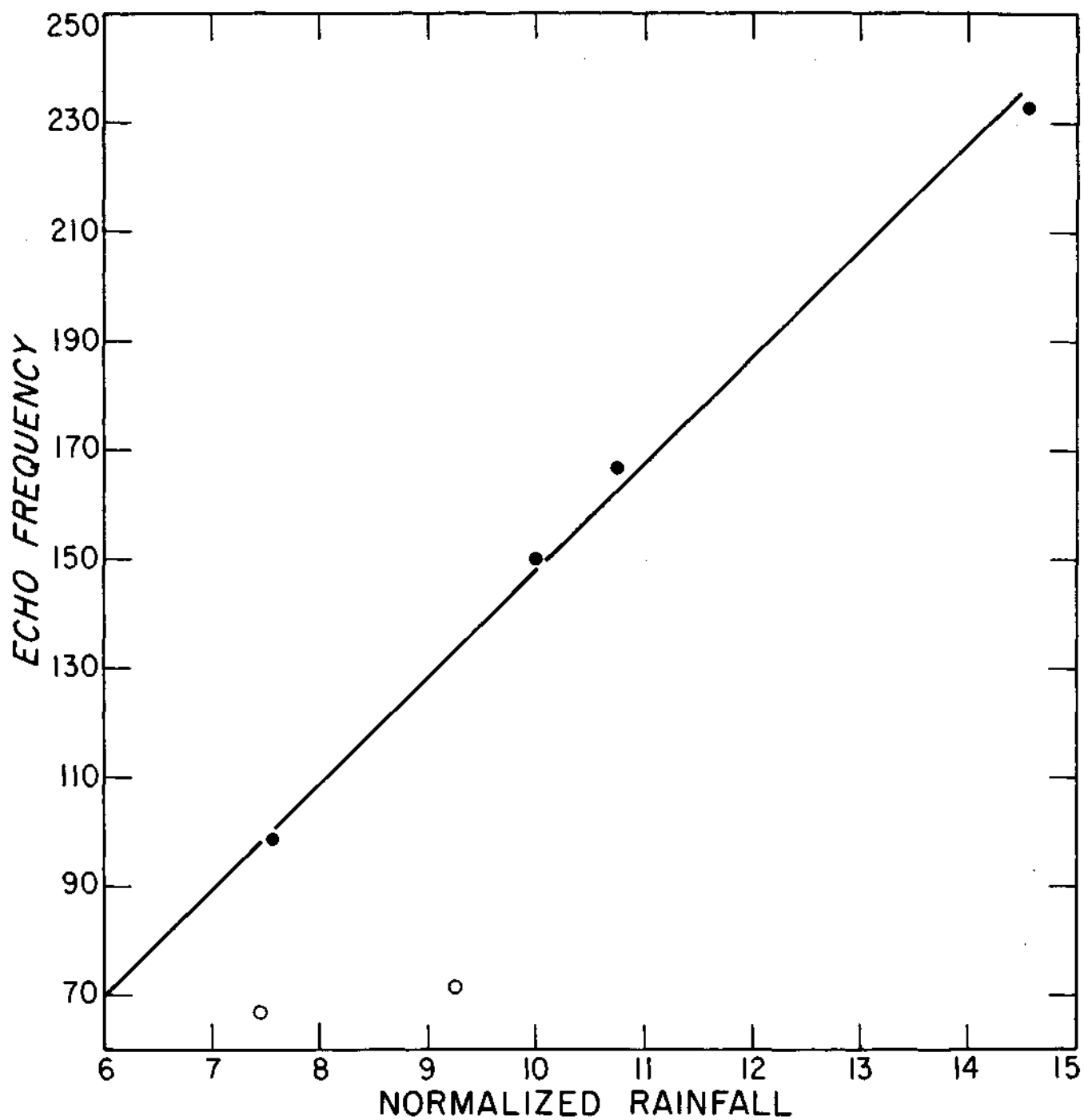


Figure 3. The relationship between echo frequency and normalized rainfall determined from the six locations shown in Figure 1.

circle data points which obviously do not fall on the best-fit curve were derived from the rainfall analysis over the ocean. The rainfall amounts were interpolated from the estimated rainfall gradient in a region where there were no raingages as indicated by the dashed lines in Figure 4. However, if it is assumed that the radar data is more accurate at the lower end of the curve than the linear interpolation of rainfall data, then the rainfall over the Hilo Bay area can be derived. The results of reanalyzing the rainfall map in this region based upon the radar data are shown by the solid lines in Figure 4.

No attempt was made to use rainfall and radar data acquired simultaneously for this study due to the lack of recording raingages in the area. Thus, the results are only applicable to the period under investigation and only for the radar data used. It is recommended that a future investigation be carried out using radar data and rainfall totals that are timewise correlated. The results would then be useful for the determination of rainfall totals for arbitrary periods of time so long as an adequate sample of echo occurrences is used.

Echo Diameter Frequency versus Range. A scale was constructed from acetate consisting of a series of circles ranging from 750 to 13,500 yards in diameter in intervals of 750 yards. The radar film was scanned for isolated echoes and the diameters were noted. A total of over 2700 echoes were measured and included in this analysis. Only those echoes which were separated by at least one diameter were assumed to be isolated for the purpose of this study.

The number of echoes contained within range intervals of 10 kiloyards were tabulated and normalized by the area within the interval. Separate tabulations were made for echoes observed over land and over the ocean. No data were obtained in the interval of 0-10 kiloyards due to ground and sea clutter. Since all of the data were obtained when the radar was operated in the split-Z mode, the elevation angle of the antenna for azimuth positions between 180° and 360° entered into the area determination. The assumption was made that echoes did not penetrate the

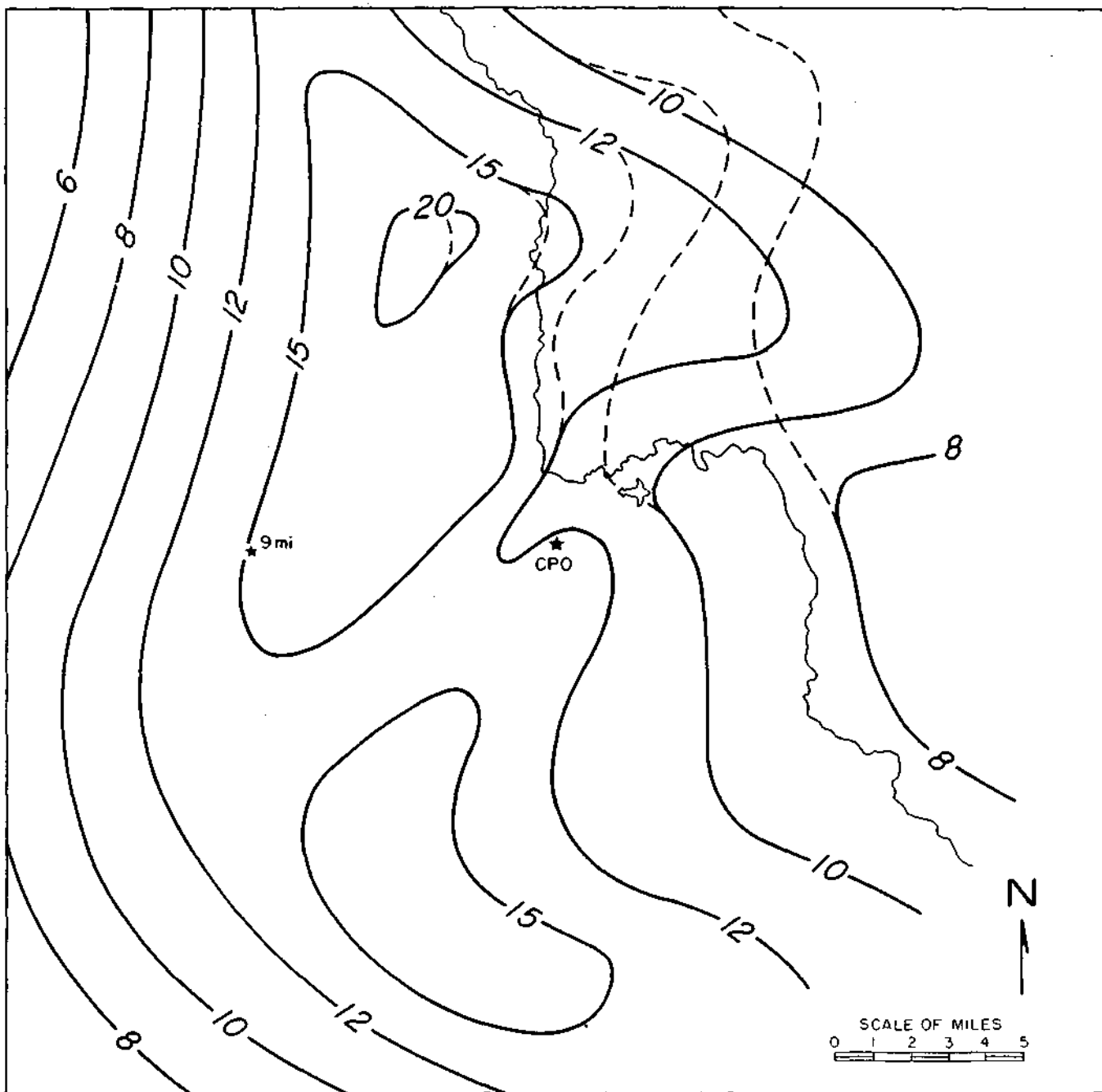


Figure 4. The isohyetal map for the period July 11 through August 24, 1965 drawn by linear interpolation of rain gauge data (dashed lines) and adjusted by echo frequency (solid lines).

trade inversion, which according to Lavoie (1966), was at a mean altitude of 2400 meters. The result of this assumption is that the radar beam sliced through the inversion at a range of approximately 34 kiloyards over land when the split-Z mode was used. The area between 30 and 40 kiloyards was adjusted to account for the antenna tilt and no over land data were tabulated beyond 40 kiloyards to the west of the radar location. However, since the antenna was at 0° elevation between 0° and 360° azimuth, all of the echo data to the 60-kiloyard range of the radar were used.

The results of the tabulations are shown in Figure 5. The abscissa is the number of echoes per square nautical mile and the ordinate is the range interval. The dotted bars represent sea echo frequency while the open bars are land echo frequency. The four graphs represent echo diameter intervals of 0-750, 750-1500, 1500-2250, and 2250-3000 yards.

The first obvious conclusion to be drawn from the data is that the most frequent size of echo observed either over land or over the ocean is contained within the 0-750 yard diameter class interval. This class interval contains nearly twice as many echoes per square mile as larger echo diameters.

The second outstanding feature shown by these data is the decreasing frequency of over-ocean echoes in all size class intervals with increasing range. This decrease cannot be accounted for by beam refraction or range effects of the radar. It simply suggests that the initial echoes appear less frequently with increasing distance from the island. The question of utmost importance to be answered then is one concerned with the influence of the island on the dynamics and thermodynamics of the sub-inversion air over the ocean in which the showers initially form.

The relative frequency of land-to-sea echoes shown in Figure 5 is two to one or greater for all range intervals. This increase in number over land may be

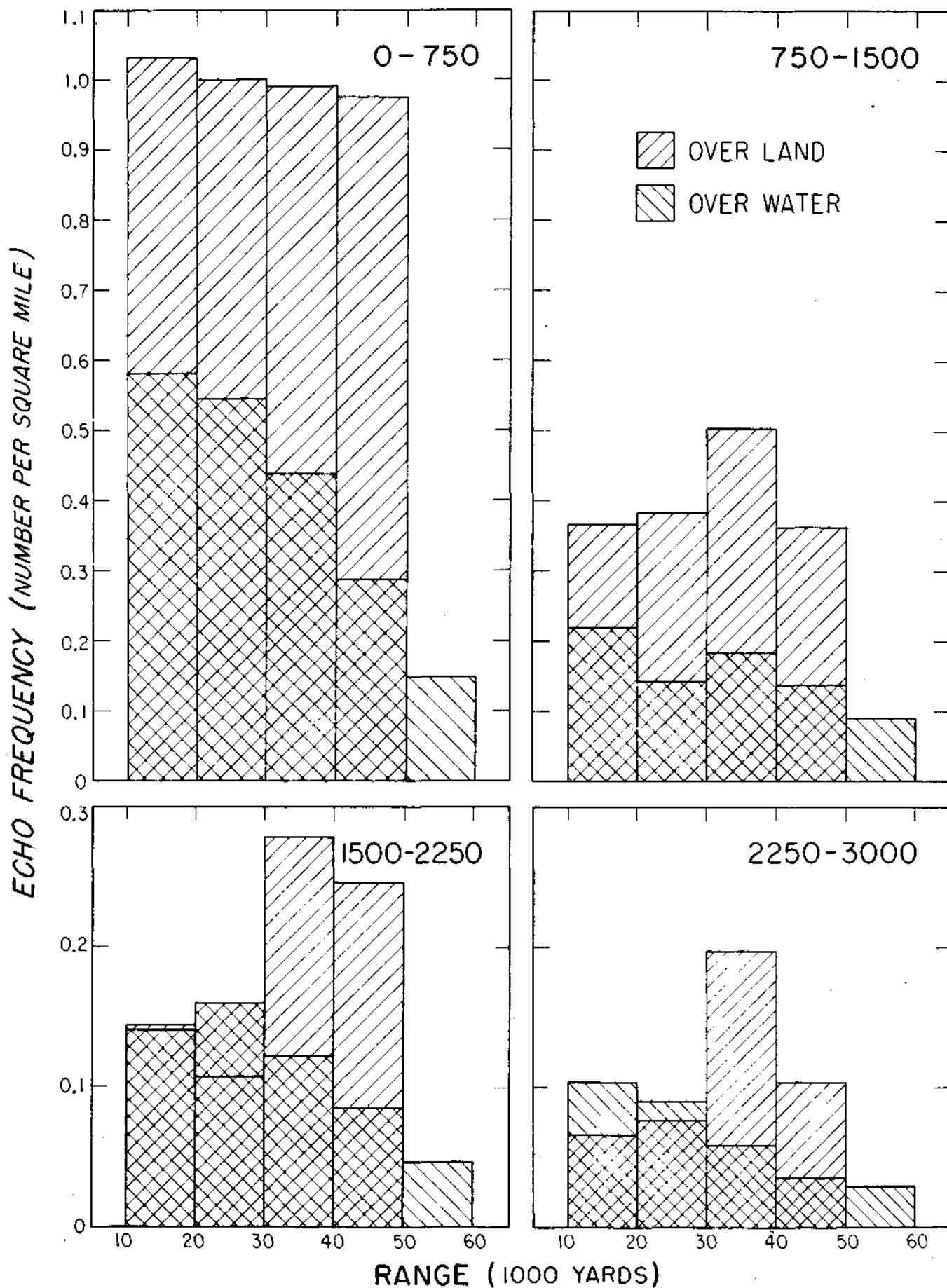


Figure 5. Normalized echo frequency relationship to range for echoes of 0-750, 750-1500, 1500-2250, and 2250-3000 yards in diameter.

attributed to the breakup of larger echo masses or the scattering of shower lines as they move inland. Many qualitative observations of this type were noted by the radar operators during the summer.

The peak in frequency seen in Figure 5 in the range interval of 30-40 kiloyards may, in part, be due to the assumption of the showers not penetrating the trade inversion. This assumption should be qualified in future studies to include the weakening or dissolution of the trade inversion, and also the possible increased height of larger diameter showers.

Initial Echo -- Movement and Origin. The radar film was carefully screened in order that the formation and movement of individual echoes could be studied in relation to the distance from the island and the prevailing trade winds. For the purpose of this study the echoes had to be completely isolated, and, of course, had to appear within range of the radar. As a result, very limited data were available since the majority of the showers appeared to be associated with organized lines or bands. However, even though the sample contains only 50 cases, some of the features of the data are supported by other studies.

Table 4 shows the number of echoes which dissipated within particular range intervals as well as their speed at the time of dissipation.

Table 4. Echo Dissipation and Speed as a Function of Range

<u>Range Interval</u> <u>(kiloyards)</u>	<u>Number of Echoes</u>	<u>Speed</u> <u>(knots)</u>
10-20	10	11.9
20-30	18	10.8
30-40	11	13.4
40-50	7	13.4
50-60	4	12.6

Once again a qualitative observation noted by the radar operators on numerous occasions, concerning the decrease in speed of individual echoes as they approach shore, has been substantiated by the average speeds shown in the above table. The average speed decrease is not large, but is indicative of the influence of the island on the motion of the trade wind showers.

The relationship between the echo velocity and the mean trade wind velocity through a depth comparable to the cloud was examined for the fifty isolated echoes. The correlation between the echo and trade wind speed and direction is shown in Figure 6. The data are quite scattered and it was not deemed worthy to determine the correlation coefficient. However, it is interesting to note that the speed of the echoes is usually greater than the trade wind speed and that the echoes tend to move to the right of the wind direction. The movement of the radar echo to the right of the environmental wind is not unique to the trade wind showers as this has been observed by others in studies of mid-latitude storms (e.g., Newton and Katz, 1958). The differential in the speeds may be due to the growth of the shower on the downwind side rather than to a true propagation of the individual cell. This explanation has also been invoked by other investigators to describe squall line echo behavior.

Typical Echo Morphology and Special Cases. As stated before, the primary purpose of the M-33 radar was to provide the other scientists with information and prognostications on the development and movement of showers. To perform this task with some degree of success required that the radar operators observe the various echo patterns very closely and then categorize them mentally for future reference. The most typical large scale pattern of echo development and movement is shown in a, b, and c of Figure 7. During a period of approximately 30 minutes, scattered echoes appear on a previously clear scope, as shown in Figure 7a, and continuously grow and dissipate with a lifetime of the order of 30 minutes. The

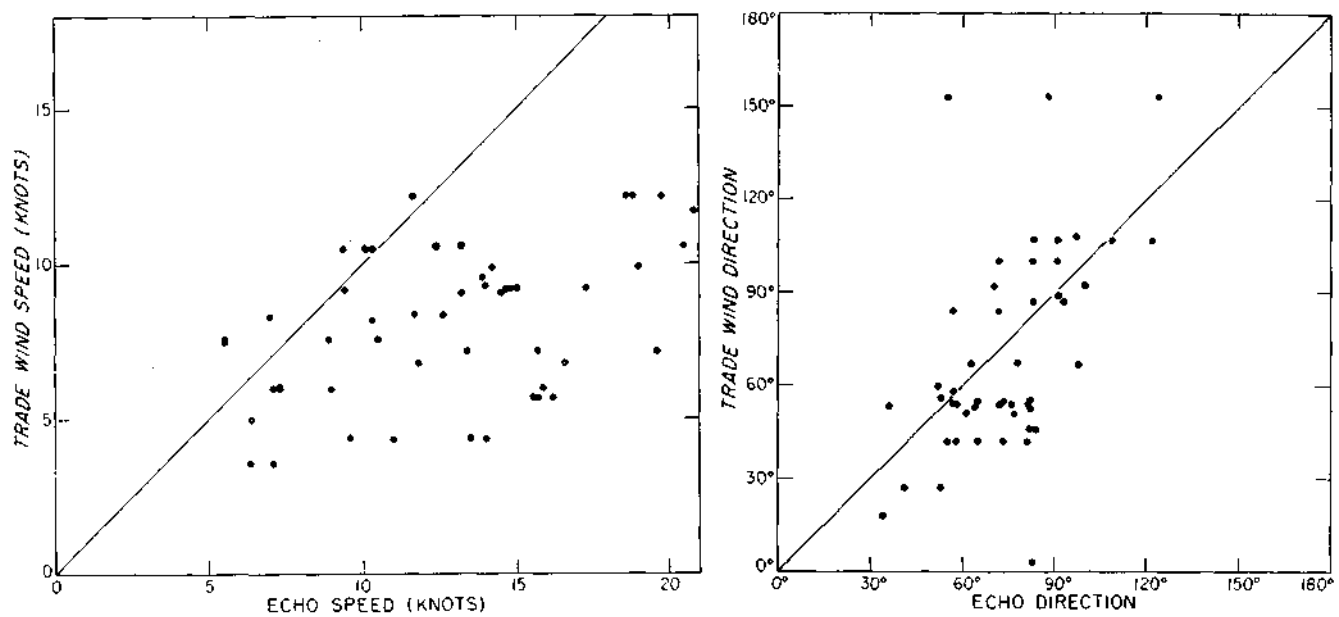
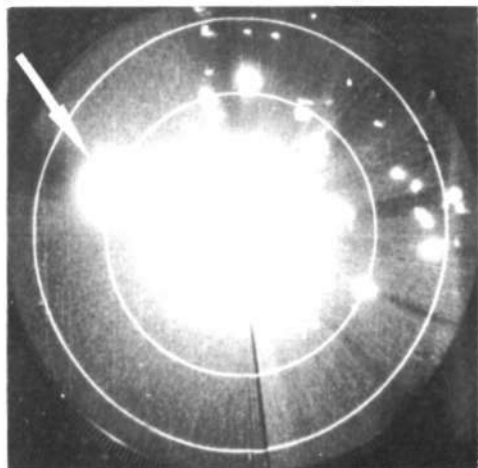


Figure 6. The relationship between echo and trade wind speed and direction.

next stage of development is the organization of the scattered cells into groups and bands as shown in Figure 7b. There may be as many as three such bands visible at the same time with a spacing of about ten miles. Such a case is illustrated in Figure 7c. The bands move inland (Figure 7c) and upon passing over the shore apparently begin to break up into individual cells. However, if the orographic cloud on Mauna Kea is developed at this time the cells merge with the steady rain and lose their identity.

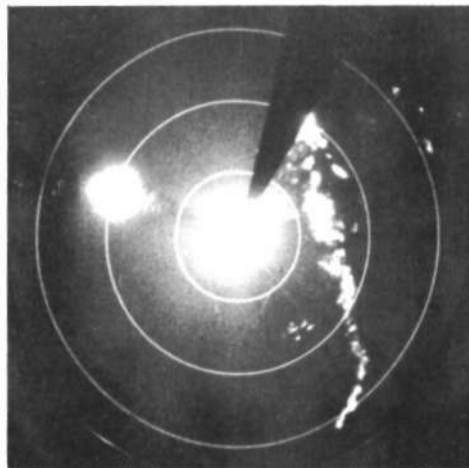
On occasion when the orographic cloud was well developed and extended to the coastline, the shower activity was inhibited within a very short distance. Such was the situation shown in Figure 7d and 7e. The second photo was taken approximately ten seconds after the first and at a reduced gain of 4db. The interesting observation in this case is the apparent spiral bands noted in the reduced gain photo. This sort of presentation may be due to the lack of convective vertical motions so that the light rain associated with the echo was subject to the wind pattern generated by the interaction of the northeast trade winds and the mountain barrier on shore.

On July 20 Mauna Kea became truly the "white mountain" with a layer of what appeared to be snow, but later was found to be small hail. Several observers reported hearing thunder and some electrical activity was noted at the Mauna Loa Observatory. In the brief period of this project, this was the only day that radar echoes were observed to move from the west across the saddle between the two large mountains. The group of echoes in the southwest quadrant of Figure 7f were associated with the hail. These echoes were moving to the northeast as was the echo noted to the northeast of Mauna Kea. Simultaneous with the movement of these echoes from the Kona side of the island, there were showers observed over Hilo Bay which were moving with the northeast trades toward land. During this period the sounding revealed that the trade inversion had all but disappeared and



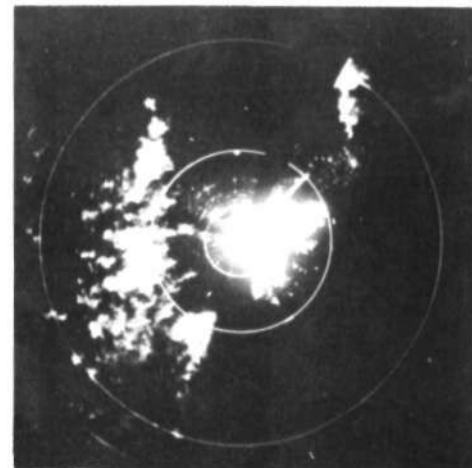
Aug 20, 65 60 Kyds

a) Widely scattered echoes over water with Mauna Kea to the northwest at 40 kiloyards range.



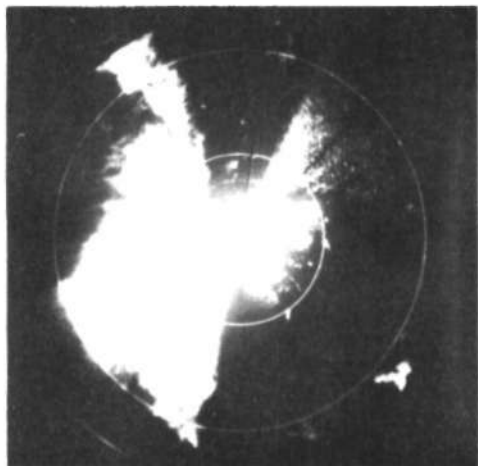
Jul 23, 65 60 Kyds

b) A line of showers which developed from echoes similar to (a).



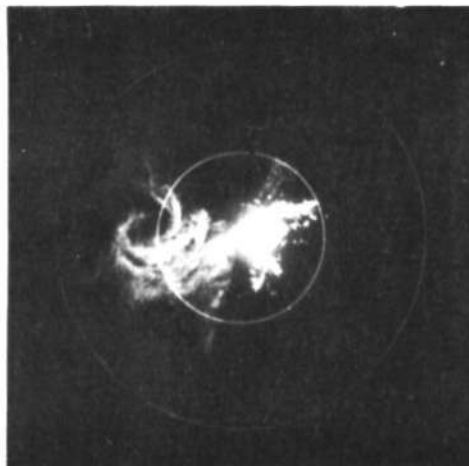
Jul 23, 65 20 Kyds

c) The remnants of a line after passing onshore and the approach of a new line from the northwest.



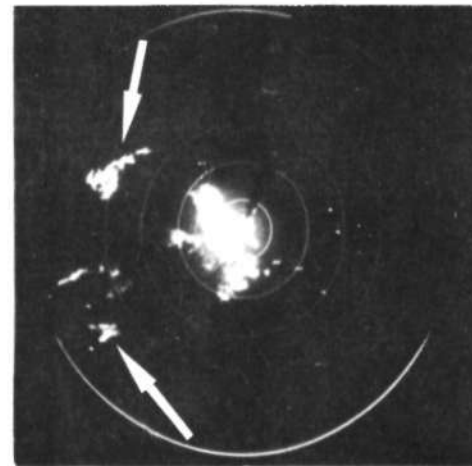
Aug 12, 65 20 Kyds

d) The remains of a line after merging with an existing orographic cloud.



Aug 12, 65 20 Kyds

e) The same as (d) but with 4 db reduced sensitivity showing a spiral banded structure in the flow pattern.



Jul 20, 65 60 Kyds

f) Kona thunderstorms which produced hail on both Mauna Kea and Mauna Loa. The antenna was tilted at a slightly greater angle than usual and the typical Mauna Kea ground return was not observed.

Figure 7. Typical patterns and special cases of echoes observed with the M-33.

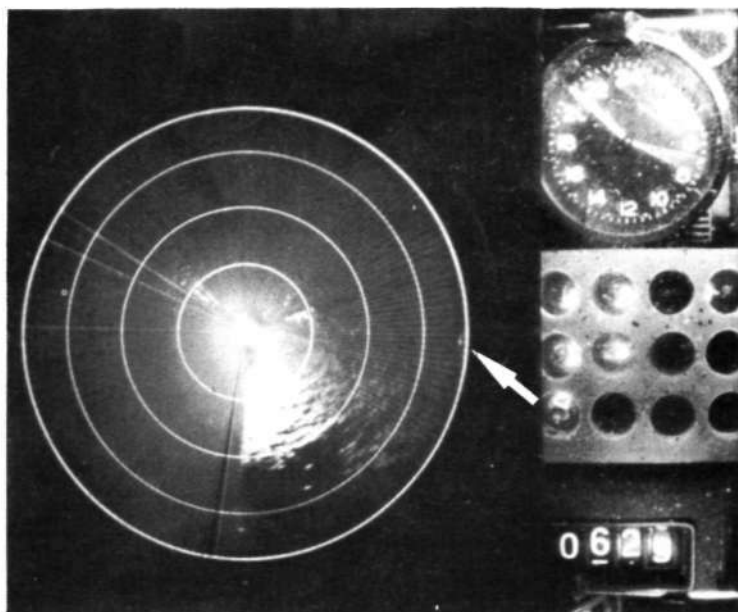
the lower layers were quite unstable. The trade winds were very light and converged with the Seabreeze from the Kona area to form the hail-producing thunderstorms observed.

It must be emphasized that these were typical and special cases which were observed during the course of a two-month program in 1965 and much additional data are needed before the radar climatology of the region will be realized. However, the limited cases discussed here certainly show the usefulness of radar observations in the study of tropical rainshowers and circulation patterns in the state of Hawaii. It is recommended that for future work a range height indicating radar be acquired which would be a very useful complement to the M-33 for cloud physics research on the warm rain mechanism.

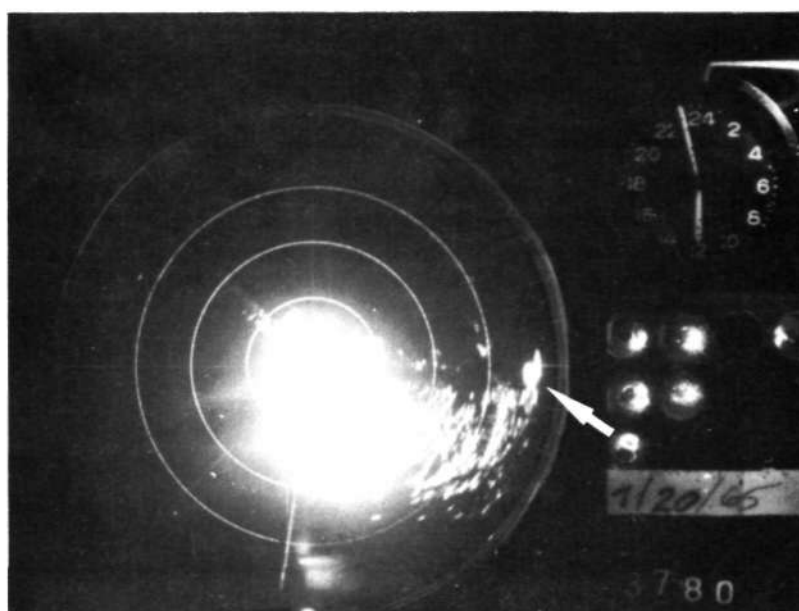
GPG-1

The GPG-1 radar was located on Mauna Kea at 2100 meters mean sea level (see Figure 1). This location proved to be undesirable because of the existence of a strong trapping layer which was frequently present below the radar's location. Figure 8 shows a comparison of ground clutter for two days of operation of this radar. Calibrations on these days indicated that the radar was operating at about the same sensitivity. If anything, the radar was slightly more sensitive on July 14- than on July 20. In both instances the antenna was depressed 3° from the horizontal. It is immediately apparent that there is much more ground return from the eastern and southeastern sections on July 20 than on July 14. In particular, attention is directed to echoes which are due east at about 15 to 20 miles. These echoes are from oil storage tanks just east of Hilo as well as other structures around Hilo. The echoes are much weaker on July 14 (at least 10db) and furthermore, are at a somewhat greater range than on July 20.

The explanation for this anomaly is believed to be the large gradient in refractive index associated with the trade inversion. Figure 9 shows the Hilo



July 14, 1965



July 20, 1965

Figure 8. Examples of differences in ground return due to the trapping gradients of the trade inversions.

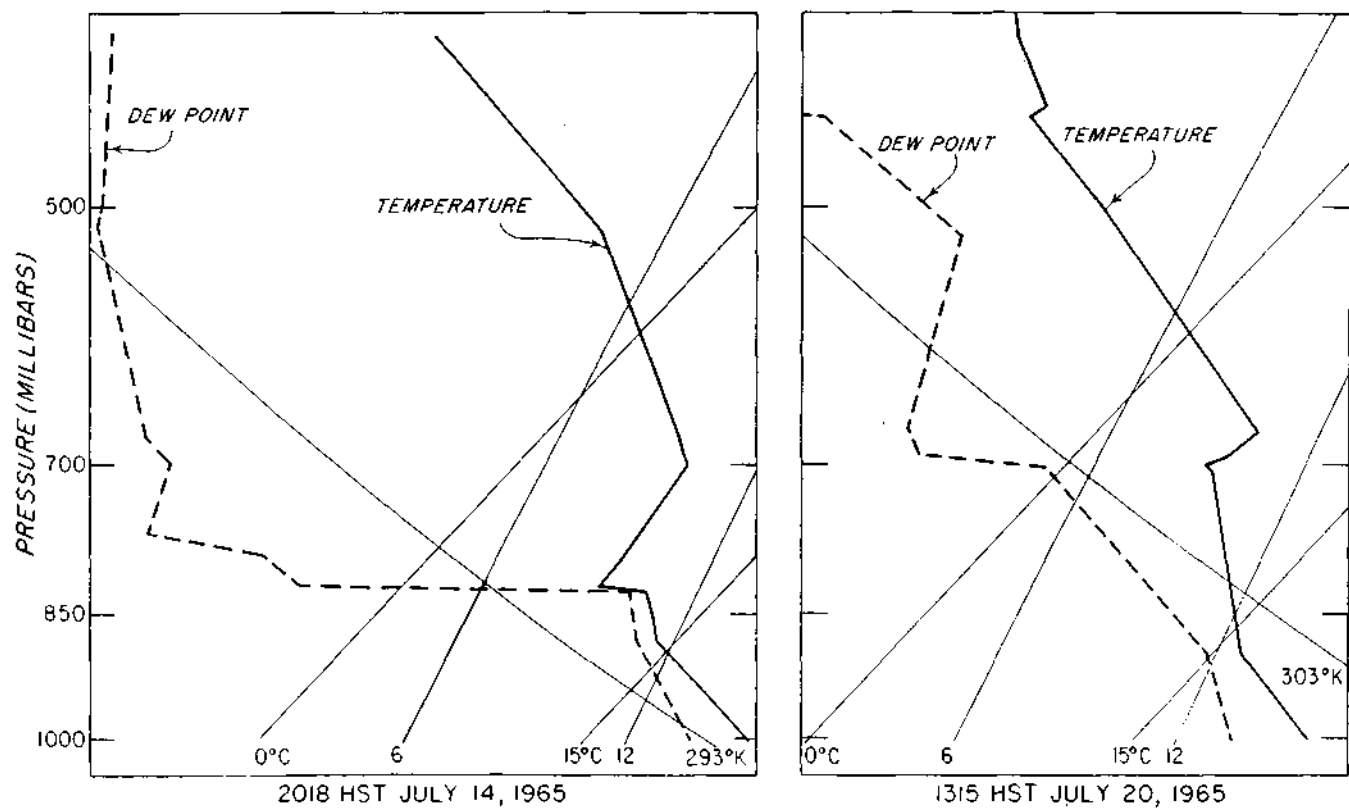


Figure 9. Radiosonde observations at Hilo, Hawaii on July 14 and July 20, 1965.

soundings for July 14 and July 20. The refractivity profiles were calculated using data from these soundings with the simplified equation for refractivity given by Bean and Dutton (1966).

$$N = \frac{77.6}{T} \left(P + \frac{4810e}{T} \right)$$

where N is the refractivity, T is the temperature in degrees Kelvin, P is the pressure in millibars and e is the vapor pressure in millibars.

The refractivity soundings are shown in Figure 10. The analysis shows that on July 14 the inversion is below the radar and on July 20 the inversion, if it exists at all, is well above the radar. The gradient on July 14 was 780 N units per kilometer. Further radiosonde analysis has shown that more than one-half of the time, refractivity gradients in excess of 150 N units per kilometer were in existence below the radar height of the GPG-1 for the period July 11 through July 31.

According to Bean and Dutton, a gradient in excess of 150 N units per kilometer produces trapping. Thus, it is not surprising to note such large differences in ground return for a gradient of 780 N units per kilometer.

This large uncertainty in the validity of data obtained from this location dictated the cessation of operation of this radar. Consequently, the GPG-1 was dismantled and removed late in July and attention was focused on the M-33 at the Cloud, Physics Observatory.

SUMMARY

Two X-band radars, a tracking M-33 and a GPG-1, were used extensively during the period July 11 through August 24, 1965 to obtain data on trade wind showers near the island of Hawaii in support of an international cloud physics program.

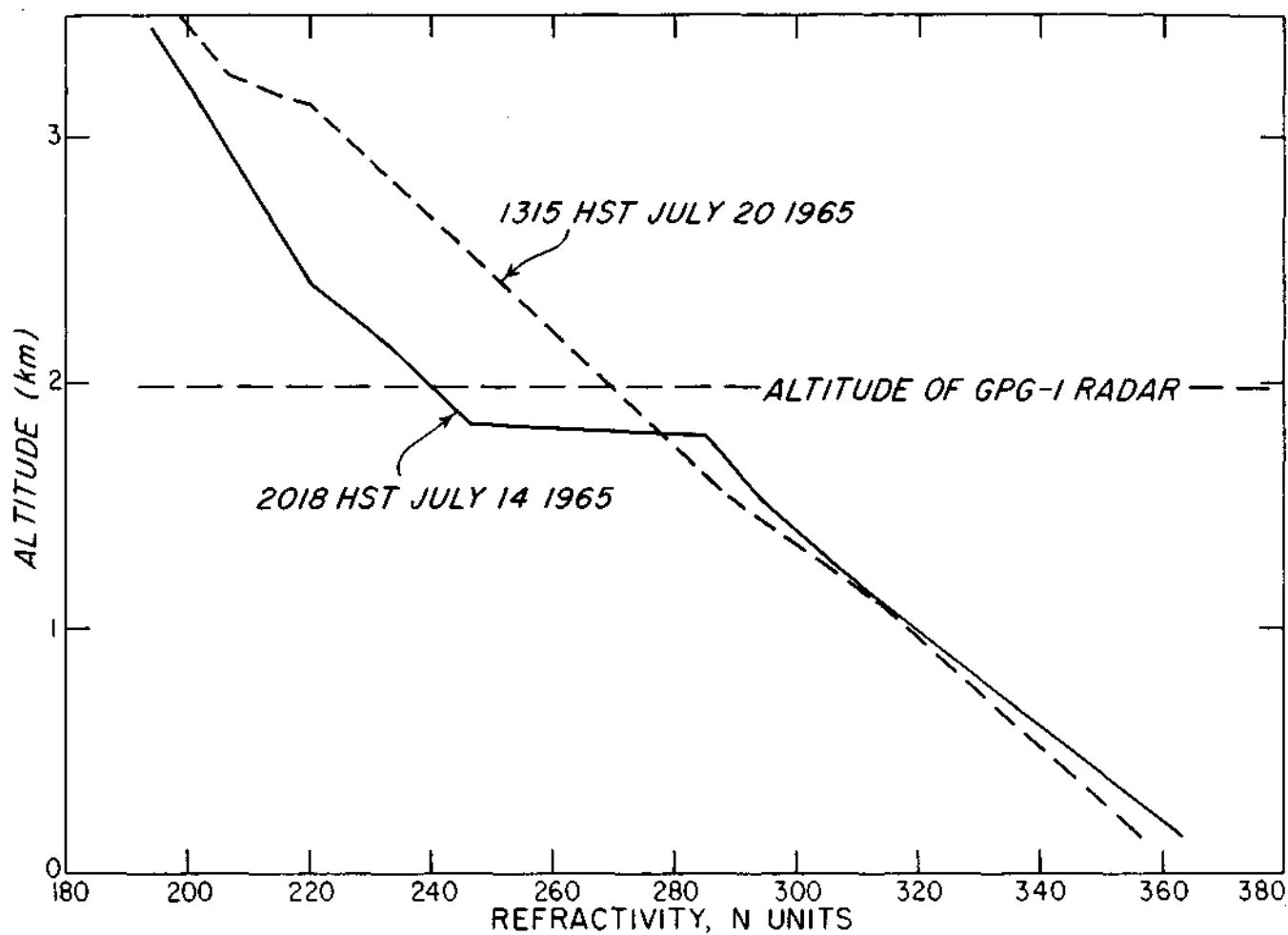


Figure 10. Refractivity soundings derived from the radiosonde observations of July 14 and July 20, 1965.

In addition, the radars were used for tracking constant level and special sounding balloons. The real time data from the M-33 was used to aid in providing short-range forecasts to cloud physicists from Japan and the United States.

The M-33 radar proved to be a valuable tool for the study of trade wind showers in Hawaii. The relationship between echo frequency and rainfall was exceptionally good for the period of the field program.

The frequency of echoes of a given diameter as a function of range is indicative of the climatology of shower evolution. These results coupled with the dependence of echo movement on the trade winds provided limited quantitative information on the development, size, and movement of trade wind showers.

The GPS-1 was operated for a brief period of time at the 2100 meters elevation on the windward slopes of Mauna Kea. Due to unfavorable atmospheric conditions at this location, the radar was returned to the CPO and full effort was devoted to the operation and maintenance of the M-33.

RECOMMENDATIONS

As a result of the experience gained during the two-month project in the summer of 1965, the following list of recommendations is presented as a guide to future work of this kind.

- 1) A more extensive radar data collection program should be initiated to include periods of 24-hour operation throughout various seasons of the year.
- 2) Complementary recording raingage data are needed to extend the studies on the quantitative measurement of rainfall by radar.

- 3) An X-band RHI radar of sensitivity equivalent to the M-33 is essential to further studies on shower initiation and development.
- 4) A separate tracking radar (another M-33) is desirable so that simultaneous tracking and PPI data can be acquired.

ACKNOWLEDGMENTS

Special thanks are due Dr. E. J. Workman and Mr. R. L. Lavoie of the University of Hawaii, who provided solutions to the many logistical problems encountered during the field project. Our thanks go to Mr. J. Tefft of the National Center for Atmospheric Research for the modification and installation of the M-33 tracking radar at the Cloud Physics Observatory. Our appreciation is also extended to Mr. A. Badua and Mr. R. Cooke for their enthusiastic response to the job of maintaining and operating the radar sets. Also our thanks to Mr. R. Busniewski of ESSA, Hilo, for his help in acquiring meteorological support data for the project.

We wish to acknowledge the help of Mr. H. C. Shipman of the Shipman Ranch and to Mr. N. Brand of the Parker Ranch in making it possible to transport and locate the GPG-1 radar on Mauna Kea.

Finally, we are deeply grateful to the citizens of the island of Hawaii for their "Aloha" spirit toward all of us during the summer which made the project enjoyable as well as successful.

REFERENCES

- Bean, B. R. and E. J. Dutton, 1966: Radio Meteorology, NBS Monograph 92,
U. S. Government Printing Office, Washington, 435 pp.
- Lavoie, R. L., 1966: The Warm Rain Project in Hilo, Hawaii, Summer 1965,
Final Rept. to N. S. F., Hawaii Institute of Geophysics, HIG-66-5,
April, 52 pp.
- Newton, C. W. and S. Katz, 1958: "Movement of Large Convective Rainstorms
in Relation to Winds Aloft," Bull. Am. Meteorol. Soc., 39, 129-136.
- Saunders, P. M. , 1965: "Some Characteristics of Tropical Marine Showers,"
J. Atmos. Sci., 22, 167-174.

APPENDIX 1

PRECIPITATION LOG

221-B-W Lanikaula Street, Hilo
(200 yards east of Science Bldg. on Univ. of Hawaii, Hilo Campus)

<u>Date</u> <u>(1965)</u>	<u>June</u>		<u>July</u>		<u>August</u>	
	<u>7a</u>	<u>7p</u>	<u>7a</u>	<u>7p</u>	<u>7a</u>	<u>7p</u>
1			.09	0	0	0
2			.12	0	.03	.01
3			.05	0	.08	
4			.05	0		
5			.06	0		
6			0	0		
7			.07	0		
8			.02	0		
9			0	0		
10			0	.32		
11			1.02	.04		
12			.07	0		
13			.06	0		
14						
15			.13	.04		
16			.12	0		
17			1.18	.75		
18			.31	.04		
19		0	.02	0		
20	1.02	.18	1.42	1.23		
21	3.8	.22	.19	.38		
22	4.6	0	.01	0		
23	0	.02	.04	.06		
24	0	0	.05	0		
25	.03	0	.21	0		
26	.01	.21	.02	0		
27	0	0	0	0		
28	.11	.12	.10	0		
29	.01	0	.05	0		
30	.02	0	.10	0		
31			.26	.01		

APPENDIX 2

M-33 Radar
University of Hawaii, Hilo

SUMMARY OF OPERATIONS
by
Illinois State Water Survey

<u>Date</u> (1965)	<u>Time</u> (HST)	<u>Max.</u> <u>Step</u>	<u>Mode</u> *	<u>Date</u> (1965)	<u>Time</u> (HST)	<u>Max.</u> <u>Step</u>	<u>Mode</u> *
6/30	1532-1627	1	1,2	7/17	1643-1757	5	1,2
7/6	1923-2340	5	1	7/19	1603-1738	3	1,2
7/7	0948-1137	1	MSG	7/20	1333-1525	8	1,2
7/8	1833-1951	1	1,2		1608-1649	5	1,2
7/9	1515-1904	8	1		1658-1727	5	1,2
	1919-2151	5	1		1741-1756	5	1,2
7/10	1515-2150	8	1	7/21	0845-0917	3	1
7/12	1626-1718	6	1,2		1045-1302	4	1
	2028-2217	4	1,2		1314-1426	4	1
7/13	0807-0840	3	1,2		1511-1718	5	1
	1640-2111	1	1,2		2046-2053	3	1
7/14	1333-1415	1	MSG		2126-2151	3	1
7/15	0505-1120	6	1,2	7/22	0745-0925	2	1,2
	1328-1340	4	1,2		1052-1154	2	1,2
	1348-1356	4	1,2		1240-1427	6	1,2
	1717-1812	4	1,2		1434-1559	4	1,2
	1836-1919	4	1,2		1704-1754	3	1,2
	1941-1945	4	1,2		1916-2208	3	1,2
7/16	0816-0914	3	1	7/23	0416-0501	6	1,2
	1205-1215	3	1		0502-0805	5	1,2
	1330-1355	3	1		0900-0905	5	1,2
	1405-1421	3	1		1000-1045	3	1,2
	1431-1513	3	1		1215-1225	3	1,2
	1538-1557	3	1		1251-1742	5	1,2
	1609-1618	3	1		1813-1955	5	1,2
	1936-2001	3	1	7/24	0446-0500	4	1
	2049-2055	3	1		1126-1129	3	1

<u>Date</u> (1965)	<u>Time</u> (HST)	<u>Max.</u> <u>Step</u>	<u>Mode*</u>	<u>Date</u> (1965)	<u>Time</u> (HST)	<u>Max.</u> <u>Step</u>	<u>Mode*</u>
7/24	1144-1155	3	1	8/8	1000-1150	8	1,2
	1530-1559	3	1		1457-1750	6	1,2
7/26	0403-0640	6	1	8/9	0823-1020	3	1,2
	0711-0821	4	1		1142-1526	8	1,2
	0933-1047	3	1		1727-2135	7	1,2
7/27	1120-1335	4	1	8/10	0412-0910	6	1,2
	1424-1735	5	1		0950-1442	8	1,2
	1736-1850	5	1	8/11	0414-0748	4	1,2
	1945-2126	3	1		1400-2321	7	1,2
7/28	0406-0428	6	1	8/12	0420-0955	6	1,2
	1554-1623	2	1	8/14	0430-1750	4	1,2
	1653-1716	6	1	8/15	0408-0950	6	1
	1816-1847	6	1		1010-1218	6	1
	1903-2043	6	1	8/16	1324-1942	3	1
	2055-2114	6	1	8/17	0420-2400	7	1
	2138-2150	6	1	8/18	0000-0729	8	1,2
					0731-2400	7	1,2
7/29	1818-1831	3	1	8/19	0000-1000	6	1
7/30	1632-2210	6	1		1305-2400	2	1
7/31	1730-1940	7	1,2	8/20	0000-0305	6	1,2
8/1	1635-1740	4	1		0335-0440	6	1,2
8/2	0443-0444	6	1	8/21	0830-0000	7	1,2
	0518-0815	6	1		0000-0008	3	1,2
	1009-1146	6	1		0315-2338	8	1,2
	1330-2017	7	1		0810-1700	6	1
8/4	1235-1241	3	1,2	8/23	0814-1158	7	1
	1242-1510	4	1,2	8/24	1310-1520	2	1
8/5	0830-1130	8	1,2		1600-2226	4	1
	1216-1310	8	1,2	8/25	1035-1215	3	1
8/6	0902-1101	6	1,2		1315-1615	5	1
	1457-1537	3	1,2	8/26	0645-0845	2	1

*1 refers to Split Z elevation program

2 refers to CAPPI program